

# Medical Image Compression using iterated graph cuts based segmentation and modified fast SPIHT encoding

S.Jagadeesh<sup>1</sup>, Dr.E.Nagabhooshanam<sup>2</sup>

<sup>1</sup>(Assoc. Prof. & Head of the Department, Electronics and Communications Engineering Department, SSJ Engineering College/ JNTU, Hyderabad, Andhra Pradesh, India)

<sup>2</sup>(Dr. Prof. & Head of the Department, Electronics and Communications Engineering Department, Sridevi Women's Engineering College/ JNTU, Hyderabad, Andhra Pradesh, India)

**Abstract**— In diagnostic MRI, it is routine to acquire multiple images of the same region of interest (ROI) with different segments. In such segments acquisition, joint Level Set Segmentation exploits the mutual information across the shared ROI for improved image quality in accelerated acquisitions with under sampling of each contrast. Transmission of such segments by encoding through lossy channel was implemented in SPIHT. The above methods having more redundancy bits and more reconstruction time during the implementation. To improve the segmentation and compression time, we are proposing modified fast SPIHT (MFSPiHT) encoding technique where interactive graph cut based segmented image is compressed using MFSPiHT and recovered in both loss less and lossy transmission mediums. Proposed method has shown better comparative results.

**Index Terms**—MRI, region of interest, Level Set Segmentation, SPIHT, interactive graph cut based segmentation.

## 1 INTRODUCTION

IMAGE segmentation is an essential tool in medical image processing and is used in various applications. For example, in medical imaging filed is used to detect multiple sclerosis lesions quantification, surgical planning, conduct surgery simulations, locate tumors and other pathologies, measure tissue volumes, brain MRI segmentation, study of anatomical structure etc. Other practical applications of image segmentation are machine vision, traffic control system; face and finger print recognition and locate objects in satellite images. Image segmentation with graph cuts technique has potential usefulness for everyday applications like image cropping and colorization along with the multi-view image stitching, video texture synthesis, image reconstruction, n-dimensional image segmentation etc.

Graph-cuts are one of the leading segmentation techniques to efficiently solve a wide variety of brain tissue identification. Energy minimization along with image smoothing is performed with the graph cuts method. Different types of algorithms such as new minimum-cut/maximum flow (min-cut/max-flow), push-relabel, augmenting paths etc. are used in graph cuts method as well as the normalized cut.

Medical images contain information critical to accurate diagnosis. As a consequence of this, it is desirable that any compression operation performed on medical images should not remove vital diagnostic information. The current preferred method for compressing medical images is through lossless coding. The current standardized lossless coders for medical imaging include JPEG lossless compression [1], the JPEG-LS compression [3] and the lossless mode of the proposed JPEG 2000 scheme [5]. The performance evaluation of different lossless medical image compression methods and their effects have been summarized in [7]. The Digital Imaging and Communication in Medicine (DICOM) [6] standard supports both the JPEG and the JPEG 2000 compression scheme. In lossy

compression, the deterioration of information may lead to mis-diagnosis. However, it is possible to allow controlled degradation of information without impeding the diagnostic information in medical images. Such an approach may be found in the SPIHT.

## 2. EXISTING METHODS

### 2.1 A Variational Level Set Approach to Segmentation

Consider the case of  $N=2$ . In this case, the image domain is partitioned into two regions  $\{\Omega_i\}_{i=1}^2$ . These two regions can be represented by the regions separated by the zero level contour of a function  $\phi$ , i.e.,  $\Omega_1 = \{\phi > 0\}$  and  $\Omega_2 = \{\phi < 0\}$ . Using Heaviside function  $H$ , the energy  $E$  Eq. (1) & (2) can be expressed as an energy in terms of  $\phi$ ,  $b$ , and  $c$  as below

$$\mathcal{E} \triangleq \int \left( \sum_{i=1}^N \int_{\Omega_i} K(\mathbf{x} - \mathbf{y}) |I(\mathbf{y}) - b(\mathbf{x})c_i|^2 d\mathbf{y} \right) d\mathbf{x} \quad \dots \text{Eqn. (1)}$$
$$\mathcal{E}(\phi, b, c) = \int \left( \sum_{i=1}^2 \int K(\mathbf{x} - \mathbf{y}) |I(\mathbf{y}) - b(\mathbf{x})c_i|^2 M_i(\phi(\mathbf{y})) d\mathbf{y} \right) d\mathbf{x} \quad \dots \text{Eqn. (2)}$$

Where  $M_1(\phi(\mathbf{x})) = H(\phi(\mathbf{x}))$  and  $M_2(\phi(\mathbf{x})) = 1 - H(\phi(\mathbf{x}))$ . In practice, a smoothed Heaviside function  $H_\epsilon(\mathbf{x}) = \frac{1}{2} [1 + \frac{2}{\pi} \arctan(\mathbf{x}/\epsilon)]$  to approximate the original Heaviside function  $H$ , with  $\epsilon=1$ . It is necessary to add a regularization term  $\mathcal{R}(\phi)$  to the above energy in the following energy functional:

$$\mathcal{F}(\phi, b, c_1, c_2) \triangleq \mathcal{E}(\phi, b, c) + \mathcal{R}(\phi) \quad \dots \text{Eqn. (3)}$$

The first term in  $R$  serves to regularize the zero level contour of  $\phi$  as in typical level set methods, while the second term regularizes the entire level set function  $\phi$  by penalizing its deviation from signed distance, as in the level set methods proposed by Li et al. The energy  $\mathcal{E}(\phi, b, c)$  is the data term in variational framework. Similarly, multiple level set functions  $\phi_1, \dots, \phi_n$  to represent regions  $\{\Omega_i\}_{i=1}^N$  with  $N=2^n$  as in [4]. For convenience, a vector valued function  $\Phi=(\phi_1, \dots, \phi_n)$  to represent the functions  $\phi_1, \dots, \phi_n$ . The energy for general multiphase formulation of our method can be defined as

$$\mathcal{F}(\phi, b, c) \triangleq \int \left( \sum_{i=1}^N \int K(x-y) |I(y) - b(x)c_i|^2 M_i(\Phi(y)) dy \right) dx + \sum_{i=1}^n \mathcal{R}(\phi_i) \quad \dots \text{Eqn. (4)}$$

Where  $M_i(\Phi)$  are functions of  $\Phi$  which are designed such that  $\sum_{i=1}^N M_i(\Phi)=1$ . The definition of  $M_i$  in the four-phase case are given. For  $N=3$  and two level set functions  $\phi_1$  and  $\phi_2$ ,  $M_1(\phi_1, \phi_2)=H(\phi_1)H(\phi_2)$ ,  $M_2(\phi_1, \phi_2)=H(\phi_1)(1-H(\phi_2))$ , and  $M_3(\phi_1, \phi_2)=1-H(\phi_1)$  to obtain a three-phase formulation.

For fixed  $c$  and  $b$ , the minimization of  $F(\phi, c, b)$  consists in solving the level set evolution equation as the gradient

$$\frac{\partial \phi}{\partial t} = - \frac{\partial \mathcal{F}}{\partial \phi} \quad \dots \text{Eqn. (5)}$$

Where  $\partial F / \partial \phi$  is the Gâteaux derivative (the first order functional derivative) of the energy  $F$ . In numerical implementation, at each iteration according to Eq. (9), the variables  $c$  and  $b$  are updated according to the following procedure. For fixed  $\phi$  and  $c$ , an optimal bias field  $b$  that minimizes  $F(\phi, c, b)$ . It can be shown that the minimize  $b$  is

$$\hat{b} = \frac{(IJ^{(1)}) * K}{J^{(2)} * K} \quad \dots \text{Eqn. (6)}$$

Where  $*$  is the convolution operation, and  $J^{(1)} = \sum_{i=1}^N c_i M_i(\phi)$  and  $J^{(2)} = \sum_{i=1}^N c_i^2 M_i(\phi)$ . For fixed  $\phi$  and  $b$ , an optimal  $c$  that minimizes  $F(\phi, c, b)$ . By some calculus manipulations, it can be shown that the minimize  $c=(c_1, \dots, c_N)$  is

$$\hat{c}_i = \frac{\int (b * K) I M_i(\phi) dx}{\int (b^2 * K) M_i(\phi) dx}, \quad i = 1, \dots, N. \quad \dots \text{Eqn. (7)}$$

It is worth noting that the expression of  $b$  in Eq. (10) with convolutions shows that  $b$  is smooth. The smoothness of  $b$  is intrinsically ensured by the data term  $E(\phi, c, b)$  in variational framework. This is a desirable advantage of this method: there is no need for imposing a smoothing term to ensure the smoothness of the bias field.

## 2.2 Interactive Graph Cuts Based Segmentation

This technique is based on powerful graph cut algorithms from combinatorial optimization. Implementation uses a new version of "max-flow" algorithm.



Fig 1 (a): Image with seeds. Fig 1 (d): Segmentation results.

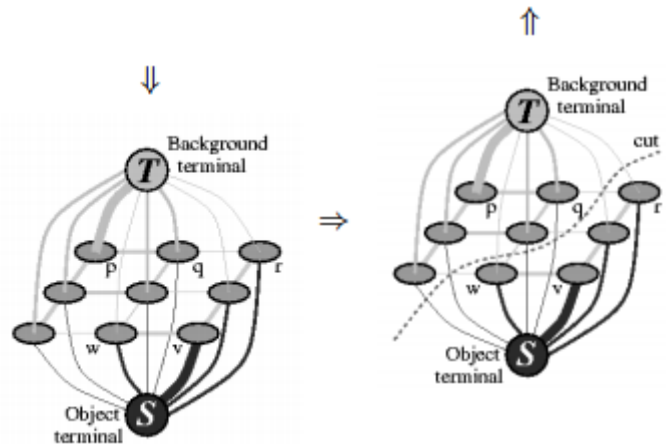


Fig 1 (b): Graph.

Fig 1 (c): Cut.

Figure 1. A simple 2D segmentation example for a  $3 \times 3$  image. The seeds are  $O = \{v\}$  and  $B = \{p\}$ . The cost of each edge is reflected by the edge's thickness. The regional term (2) and hard constraints (4,5) define the costs of t-links. The boundary term (3) defines the costs of n-links. Inexpensive edges are attractive choices for the minimum cost cut. Assume that  $O$  and  $B$  denote the subsets of pixels marked as "object" and "background" seeds. Naturally, the subsets  $O \subset P$  and  $B \subset P$  are such that  $O \cap B = \emptyset$ . Remember that to compute the global minimum of (1) among all segmentations  $A$  satisfying hard constraints

$$\begin{aligned} \forall p \in O, \quad A_p &= \text{"obj"} \\ \forall p \in B, \quad A_p &= \text{"bkg"} \end{aligned} \quad \dots \text{Eqn. (8)}$$

The general work flow is shown in Figure 1. Given an image (Figure 1(a)) we create a graph with two terminals (Figure 1(b)). The edge weights reflect the parameters in the regional (2) and the boundary (3) terms of the cost function, as well as the known positions of seeds in the image. The next step is to compute the globally optimal minimum cut (Figure 1(c)) separating two terminals. This cut gives segmentation (Figure 1(d)) of the original image. In the simplistic example of Figure 1 the image is divided into exactly one "object" and one "background" regions. To segment a given image a graph  $G = hV, E_i$  with nodes corresponding to pixels  $p \in P$  of the image. There are two additional nodes: an "object" terminal (a source  $S$ ) and a "background" terminal (a sink  $T$ ). Therefore

$$V = P \{S, T\}.$$

### 2.3 Set Partitioning In Hierarchical Trees (SPIHT)

SPIHT is the wavelet based image compression method. It provides the Highest Image Quality, Progressive image transmission, fully embedded coded file, Simple quantization algorithm, fast coding/decoding, completely adaptive, Lossless compression, Exact bit rate coding and Error protection. SPIHT makes use of three lists - the List of Significant Pixels (LSP), List of Insignificant Pixels (LIP) and List of Insignificant Sets (LIS). These are coefficient location lists that contain their coordinates. After the initialization, the algorithm takes two stages for each level of threshold - the sorting pass (in which lists are organized) and the refinement pass (which does the actual progressive coding transmission). The result is in the form of a bit stream. It is capable of recovering the image perfectly (every single bit of it) by coding all bits of the transform. However, the wavelet transform yields perfect reconstruction only if its numbers are stored as infinite imprecision numbers.

## 3 PROPOSED METHOD OF IMAGE COMPRESSION

In our proposed method, we had taken modified graph cuts algorithm and modified fast improved SPIHT. In the original graph cuts algorithm, the segmentation is directly performed on the image pixels. There are two problems for such a processing. First, each pixel will be a node in the graph so that the computational cost will be very high; second, the segmentation result may not be smooth, especially along the edges. These problems can be solved by introducing some low level image segmentation techniques, such as watershed and mean shift, to graph cuts. We choose to use mean shift for initial segmentation because it produces less over-segmentation and has better edge preservation.

Wavelet transform image coding using SPIHT Traditional

SPIHT has the advantages of embedded code stream structure, high compression rate, low complexity and easy to implement. Improved SPIHT algorithm mainly makes the following changes.

- SPIHT codes four coefficients and then shifts to the next four ones.
- When computing the maximum threshold, the improved algorithm can initialize the maximum of every block.
- The coefficients in non-important block will be coded in next scanning process or later, rather than be coded in the present scanning process .
- Our algorithm encodes the sub band pixels by performing initialization and a sequence of sorting pass, refinement pass and quantization-step updating. However, differences of initialization and sorting pass still exist between the improved SPIHT [3] and traditional SPIHT.

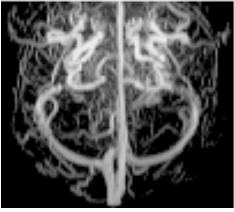
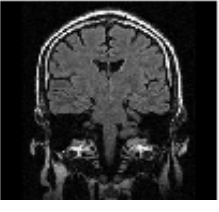
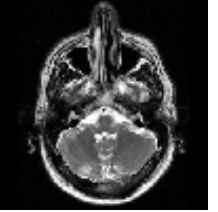

### 3.1 FLOW CHART OF PROPOSED METHOD

We had taken MR images for our method implementation,

- Step 01: Read input image; convert that image in to gray image.
- Step 02: Apply that image to segmentation process.
- Step 03: Extract the segmented image.
- Step 04: Compress the extracted image using MFSPIHT.
- Step 05: Extract the compressed image.
- Step 06: Perform inverse MFSPIHT
- Step 07: Reconstruct the original image.

Patient's data which we had taken for analysis are tabulated in table 1.

Table 1 Patient's data.

	Patient 01	Patient 02	Patient 03	Patient 04
Scan MR image				
Part of MR image	pca_brain_mri_venography_transverse_mip.png	brain_mri_coronal_flair_001.jpg	brain_mri_transversal_t2_001.jpg	circle_of_willis_mip_transverse_1.png
Size of MR image	143KB	26.7 KB	25.8 KB	143KB

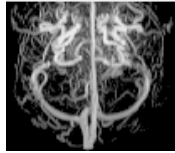
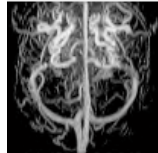
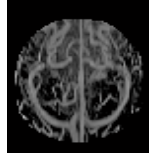

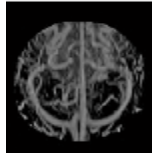


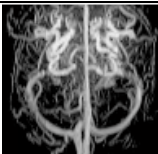
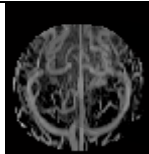
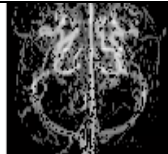
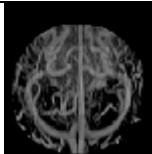

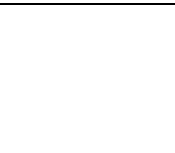

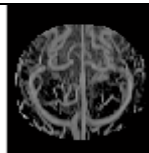


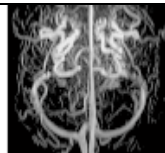

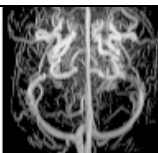
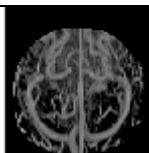

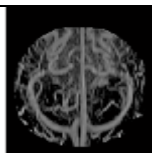
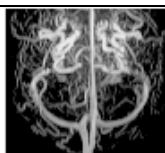
**4 Results and Discussions**

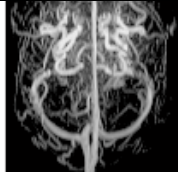
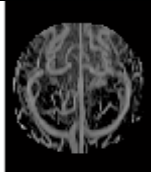
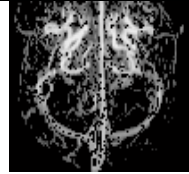
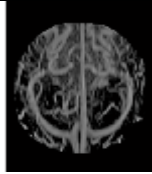
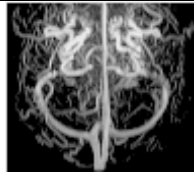
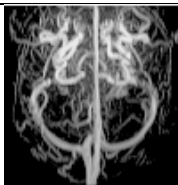
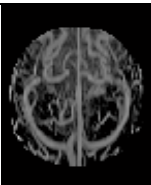
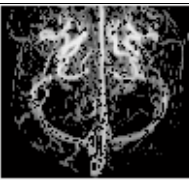
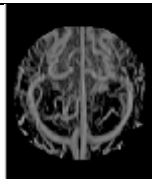

We had compared our proposed method with

1. Set Partitioning in Hierarchical Trees (SPIHT)
2. A Variational Level Set Approach to Segmentation (VLSAS)
3. Interactive Graph Cuts based segmentation (IGCS)
4. VLSAS through SPIHT (VLSSPIHT)
5. IGCS through SPIHT (IGCSSPIHT)-Our proposed method

Comparative results for Patient 01 Image tabulated in Table 2.

Table 2 Comparative Results: Patient 01

Input Image Patient 01	SPIHT	VLSAS	IGCS	VLSSPIHT	IGCSSPIHT
					
BPP	0.1	0.1	0.1	0.1	0.1
PSNR	29.57	12.86	15.24	12.84	37.69
MSE	71.70	3363.3	1944.47	3380.42	11.0666
BER	0.74	0.67	0.26	0.73	0.63
SSIM	0.86	0.76	0.73	0.70	0.92
CR	1	1	1	0.40	0.35
					
BPP	0.2	0.2	0.2	0.2	0.2
PSNR	34.08	12.86	15.24	12.83	40.91
MSE	25.38	3363.6	1944.47	3382.9	5.26
BER	0.69	0.67	0.26	0.70	0.58
SSIM	0.90	0.76	0.73	0.73	0.95
CR	1	1	1	0.40	0.35
					
BPP	0.4	0.4	0.4	0.4	0.4
PSNR	39.02	12.86	15.24	12.84	43.33
MSE	8.18	3363.67	1944.47	3381.03	3.01
BER	0.61	0.67	0.26	0.69	0.54
SSIM	0.95	0.76	0.73	0.74	0.96
CR	1	1	1	0.40	0.35
					

BPP	0.6	0.6	0.6	0.6	0.6
PSNR	41.51	12.86	15.24	12.84	43.94
MSE	4.58	3363.67	1944.47	3381.01	2.62
BER	0.58	0.67	0.26	0.69	0.55
SSIM	0.96	0.76	0.73	0.74	0.96
CR	1	1	1	0.40	0.35
					
BPP	0.8	0.8	0.8	0.8	0.8
PSNR	43.24	12.86	15.24	12.84	44.15
MSE	3.07	3363.6	1944.47	3380.88	2.50
BER	0.55	0.67	0.26	0.69	0.55
SSIM	0.97	0.76	0.73	0.74	0.96
CR	1	1	1	0.40	0.35
					
BPP	1	1	1	1	1
PSNR	44.73	12.86	15.24	12.84	44.29
MSE	2.18	3363.67	1944.47	3380.57	2.41
BER	0.53	0.67	0.26	0.69	0.56
SSIM	0.97	0.76	0.73	0.74	0.96
CR	1	1	1	0.40	0.35

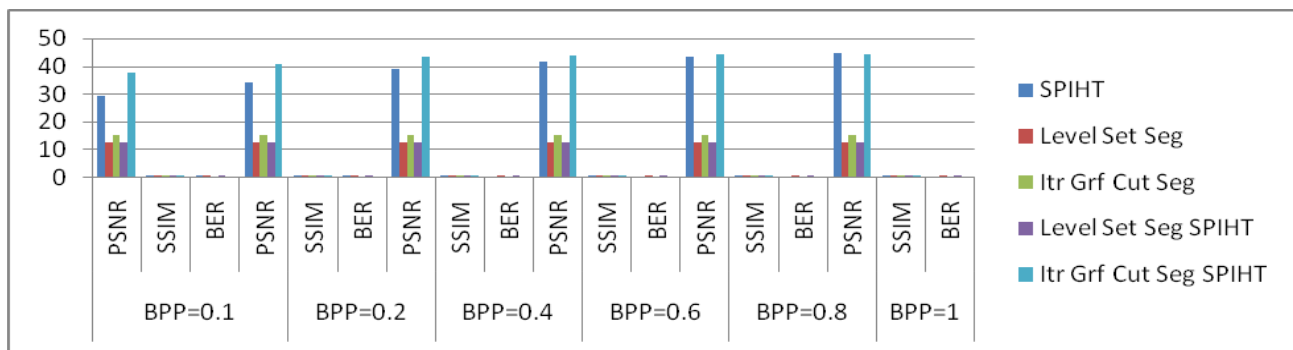
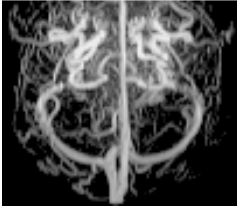
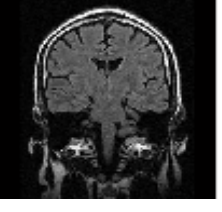
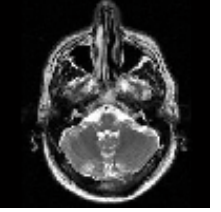



Figure 2: Comparative Results: Patient 01 with different BPP values.

Comparative results for Patient 01 Image, Patient 02 Image, Patient 03 Image and Patient 04 Image tabulated in Table 3.

Table 3 Comparative Results: Patient 01, Patient 02, Patient 03 and Patient 04 with BPP=0.6.

Method / Q.Metrics	BPP=0.6			BPP=0.6			BPP=0.6			BPP=0.6		
	PSNR	BER	SSIM	PSNR	BER	SSIM	PSNR	BER	SSIM	PSNR	BER	SSIM

Input Image	Patient 01			Patient 02			Patient 03			Patient 04		
												
SPIHT	41.51	0.58	0.96	37.42	0.71	0.94	37.36	0.69	0.88	34.77	0.88	0.97
VLSAS	12.86	0.67	0.76	16.80	0.79	0.68	16.36	0.75	0.68	5.09	0.92	0.55
IGCS	15.24	0.26	0.73	17.86	0.32	0.67	16.71	0.35	0.64	3.57	0.62	0.37
VLSSPIHT	12.84	0.69	0.74	16.69	0.79	0.66	16.23	0.76	0.67	5.11	0.96	0.53
IGCSSPIHT	43.94	0.55	0.96	37.38	0.68	0.96	36.15	0.69	0.90	39.26	0.82	0.97

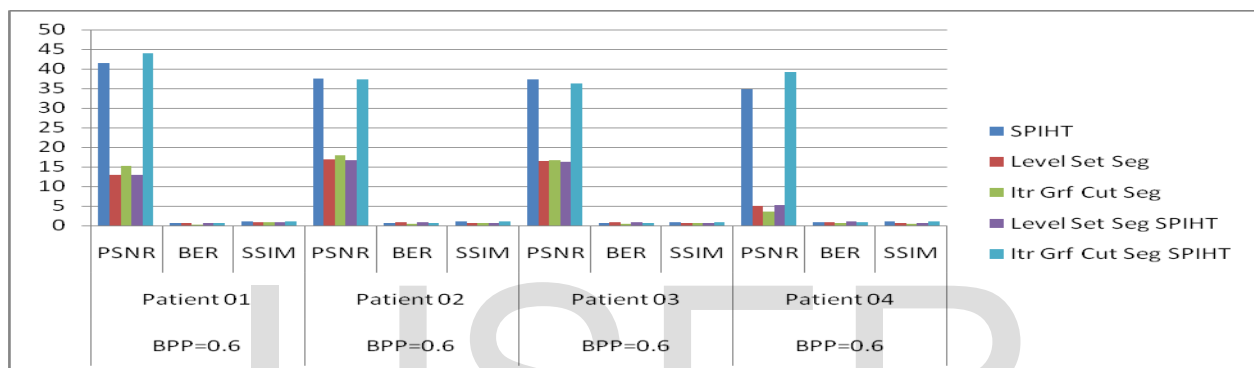


Figure 3: Comparative Results: Patient 01, Patient 02, Patient 03 and Patient 04 with different BPP=0.6 values.

From the above comparative results, using our method a segmented image can be compressed. Compressed image can be reconstructed with minimum 50 % accuracy.

## 5 Conclusions

Our proposed modified Interactive Graph Cuts based segmentation (IGCS) algorithm can be applicable to low resolution MR images; segmented image shows better segmentation comparatively. And modified fast Set Partitioning in Hierarchical Trees (SPIHT) had shown better results for high compression. Our proposed algorithm had shown better results by combining low resolution segmentation and high compression. An efficient segmented compression technique for MR Images is proposed in our algorithm.

## 6 Future Research

Our proposed method can be further applicable to improve the memory size of compressed image. CT images and DICOM Images can also be compressed using our proposed algorithm. Using our method, hardware implementation for proposed algorithm becomes flexible and easy. Further our

proposed algorithm can be applicable to high speed image decoding techniques where high scalable images are required.

## REFERENCES

- [1] Wells, W., Grimson, E., Kikinis, R., Jolesz, F.: *Adaptive segmentation of MRI data*. IEEE Trans. Med. Image. 15(4), 429–442 (1996)
- [2] Vovk, U., Pernus, F., Likar, B.: *A review of methods for correction of intensity in homogeneity in mri*. IEEE Trans. Med. Image. 26(3), 405–421 (2007)
- [3] Lewis, E., Fox, N.: *Correction of differential intensity in homogeneity in longitudinal MR images*. Neuro image 23(3), 75–83 (2004)
- [4] Dawant, B., Zijdenbos, A., Margolin, R.: *Correction of intensity variations in MR images for computer-aided tissues classification*. IEEE Trans. Med. Image. 12(4), 770–781 (1993)
- [5] Meyer, C., Bland, P., Pipe, J.: *Retrospective correction of intensity in homogeneities in MRI*. IEEE Trans. Med. Image. 14(1), 36 (1995)
- [6] Sled, J., Zijdenbos, A., Evans, A.: *A nonparametric method for automatic correction of intensity no uniformity in MRI data*. IEEE Trans. Med. Imaging 17(1), 87–97 (1998)
- [7] Leemput, K., Maes, F., Vandermeulen, D., Suetens, P.: *Automated model-based bias field correction of MR images of the brain*. IEEE Trans. Med. Image. 18(10), 885–896 (1999)

IJSER